

FEA Modeling of Material Removal Rate in Electrical Discharge Machining of Al6063/SiC Composites

U. K. Vishwakarma , A. Dvivedi and P. Kumar

Abstract—Metal matrix composites (MMC) are generating extensive interest in diverse fields like defense, aerospace, electronics and automotive industries. In this present investigation, material removal rate (MRR) modeling has been carried out using an axisymmetric model of Al-SiC composite during electrical discharge machining (EDM). A FEA model of single spark EDM was developed to calculate the temperature distribution. Further, single spark model was extended to simulate the second discharge. For multi-discharge machining material removal was calculated by calculating the number of pulses. Validation of model has been done by comparing the experimental results obtained under the same process parameters with the analytical results. A good agreement was found between the experimental results and the theoretical value.

Keywords—Electrical Discharge Machining, FEA, Metal matrix composites, Multi-discharge

NOMENCLATURE

| | |
|------------------|--|
| EDM | Electrical discharge machining |
| MRR | Material removal rate (mm^3/min) |
| NOP | Number of pulses |
| PRMMC | Particle reinforced metal matrix composite |
| P | Fraction of heat input |
| V | Voltage (V) |
| I | Current (A) |
| Q(r) | Heat flux (W/m^2) |
| R | Spark radius (μm) |
| r | Radial coordinate of the workpiece |
| K | Thermal conductivity (W/mK) |
| T | Temperature variable (K) |
| T_0 | Initial temperature (K) |
| T_{on} | Spark-on time (μs) |
| T_{off} | Spark-off time (μs) |
| x,y | Cartesian coordinate |
| C_p | Specific heat (J/kgK) |
| C_v | Crater volume (μm^3) |
| h_f | Coefficient of heat transfer of dielectric fluid |
| h_a | Coefficient of heat transfer of air |

I. INTRODUCTION

In the present scenario there is a gradual growth of different types of material like composites, ceramics.

U. K. Vishwakarma is with Mechanical and Industrial Engineering Department, Indian Institute of Technology Roorkee, Roorkee-247667, INDIA. (phone: +917417035055; fax: +91-1332-285665; e-mail: umeshvish@rediffmail.com).

A. Dvivedi is with Mechanical and Industrial Engineering Department, Indian Institute of Technology Roorkee, Roorkee-247667, INDIA (e-mail: akshaydvivedi@gmail.com).

P. Kumar is with the Mechanical and Industrial Engineering Department, Indian Institute of Technology Roorkee, Roorkee-247667, INDIA (e-mail: kumarfme@gmail.com).

These materials possess some specific material properties like strength to weight ratio. These materials have better mechanical properties than alloys, so machining them is a cumbersome task because of high tool wear rate.

The definition of composites can be restricted to include only those materials that contain reinforcement supported by a binder (matrix) material [1]. Thus, composites typically have a discontinuous reinforcement or particle phase that is stiffer and stronger than the continuous matrix phase. These advanced composites are considered to be an excellent candidate for high temperature structural materials [2].

An Aluminium alloy with SiC reinforcement has replaced the conventional materials in aerospace, automobile and automotive industries [3]. Li et al. [4] showed that the SiC reinforcing particles have the strongest effect on improving the strength of the composite as compared to other ceramic particles (Cr_3C_2 , TiC and Ti(C, N)). SiC reinforcing particles exhibits higher fracture toughness and hardness as well as a limited decomposition to increase matrix strength. In contrast to high tool wear and high cost of tooling with conventional machining, noncontact material removal process offers an attractive alternative [5, 6]. Among the non-conventional machining methods EDM has proved to be the most prominent machining method to machine composite materials. Muller et al. [7] investigated material removal mechanism of EDM and laser cutting while machining AA2618-20%SiCp and A356-35%SiCp with Cu tool electrode. Both processes proved to be suitable for machining PRMMCs, laser provides significant advantages in terms of removal rate. EDM however induced less thermal damage than that was observed using the laser. Dhar et al. [8] developed a second order, non-linear mathematical model for establishing the relationship among machining parameters. Kanagarajan et al. [9] also developed a statistical models based on second order polynomial equations for the optimization of different process characteristics, using non-dominated sorting genetic algorithm (NSGA-II). Witold et al. [10] presented a FEA model to predict the thermal stresses induced during the cooling of Cr- Al_2O_3 composite processed by sintering. Mandal et al. [11] developed a mathematical model using regression analysis to predict the wear behavior of the MMCs. The wear of MMC is much lesser in comparison with hardened; tempered AISI 4340 steel.

Literature reports extensive studies on various aspects of EDM process, but very less attention has been given to FEA modelling of EDM process for MMC. There are certain

difficulties involved in the modelling of MMC's like, macroscopic combination of two or more distinct materials having a recognizable interface between them, non-uniform distribution due to improper mixing etc.

In the present investigation a FEA model has been developed, for single discharge EDM. Different aspects of machining have been considered like pulse-on time, pulse-off time, number of pulses, spark gap etc. Further, the single discharge model has been extended to predict the temperature distribution for second discharge. Later, the predicted results obtained from the model have been verified with the experimental results and very good co-efficient of correlation has been found between predicted and experimental results.

II. THERMAL MODEL OF EDM

In EDM of Al6063/SiC composite, the matrix material melts at a relatively low temperature, but the temperature rise is insufficient for reinforced particles to melt. After melting of matrix, in the absence of matrix material the reinforcement evacuates from the crater without getting melted. The mode of heat transfer in solid is through conduction and between the dielectric and workpiece is through convection. The following assumptions are made in the present analysis to make problem mathematically feasible:

A. Assumptions

- The workpiece domain is considered to be axisymmetric.
- The composition of workpiece material is quasi-homogeneous.
- The heat transfer to the workpiece is by conduction.
- Inertia and body force effects are negligible during stress development.
- The workpiece material is elastic-perfectly plastic and yield stress in tension is same as that in compression.
- The initial temperature was set to room temperature in single discharge analysis.
- Analysis is done considering 100% flushing efficiency.
- The workpiece is assumed as stress-free before EDM.
- The thermal properties of workpiece material are considered as a function of temperature. It is assumed that due to thermal expansion, density and element shape are not affected.
- The heat source is assumed to have Gaussian distribution of heat flux on the surface of the workpiece.

B. Governing Equation

The governing heat transfer differential equation without internal heat generation written in a cylindrical coordinates of an axis symmetric thermal model for calculating the heat flux is given by [12].

$$\rho C_p \left[\frac{\partial T}{\partial t} \right] = \left[\frac{1}{r} \frac{\partial}{\partial r} \left(K_r \frac{\partial T}{\partial r} \right) + \frac{\partial}{\partial z} \left(K \frac{\partial T}{\partial z} \right) \right] \quad (1)$$

Where ρ is density, C_p is specific heat, K is thermal conductivity of the workpiece, T is temperature, t is the time and r & z are coordinates of the workpiece.

C. Heat Distribution

Plasma channel incident on the workpiece surface causes the temperature to rise in the workpiece. The distribution of plasma channel can be assumed as uniform disk source [13]-[16] or Gaussian heat distribution [17]-[21], for EDM. Gaussian distribution of heat flux is more realistic and accurate than disc heat source. Fig. 1 shows the schematic diagram of thermal model with the applied boundary conditions.

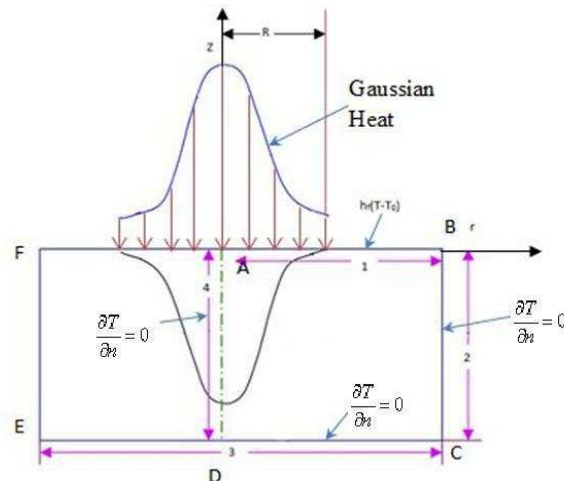


Fig. 1 An axisymmetric model for the EDM process simulation

D. Boundary Conditions

The workpiece domain is considered to be axisymmetric about z axis. Therefore taking this advantage, analysis is done only for one small half (ABCD) of the workpiece. The workpiece domain considered for analysis is shown in Fig. 1. It is clearly evident from Fig. 1 that the maximum heat input will be at point A.

On the top surface, the heat transferred to the workpiece is shown by Gaussian heat flux distribution. Heat flux is applied on boundary 1 upto spark radius R , beyond R convection takes place due to dielectric fluids. As 2 & 3 are far from the spark location no heat transfer conditions have been assumed for them. For boundary 4, as it is axis of symmetry the heat transfer is zero.

In mathematical terms, the applied boundary conditions are given as follows:

$$K \frac{\partial T}{\partial z} = Q(r), \text{ when } R < r \text{ for boundary 1}$$

$$K \frac{\partial T}{\partial z} = h_f (T - T_0), \text{ when } R \geq r \text{ for boundary 1}$$

$$\frac{\partial T}{\partial n} = 0, \text{ at boundary 2, 3 \& 4.}$$

where h_f is heat transfer coefficient of dielectric fluid, $Q(r)$ is heat flux due to the spark and T_0 is the initial temperature.

E. Material Properties

The material properties of matrix and reinforcement are given in Table I and Table II respectively.

F. Heat Flux

A Gaussian distribution for heat flux [21] is assumed in present analysis.

$$Q(r) = \frac{4.45 PVI}{\pi R^2} \exp \left\{ -4.5 \left(\frac{r}{R} \right)^2 \right\} \quad (2)$$

where P is the percentage heat input to the workpiece, V is the discharge voltage, I is the current and R is the spark radius. Earlier many researchers have assumed that there is no heat loss between the tool and the workpiece. But Yadav et al. [21] have done experiment on conventional EDM and calculated the value of heat input to the workpiece to be 0.08. Shankar et al. [22] calculated the value of P about 0.4-0.5 using water as dielectric.

G. Spark Radius

During the spark-on time the size of plasma does not remain constant but it grows with time [17], mainly depends upon electrode material and polarity. DiBitonto et al. [17] have calculated the radius of plasma discharge channel in the form of integral equation for rectangular pulses. Erden [23] further integrated this equation and found that the radius of discharge channel depends upon the discharge power and time as given in (2).

$$R(t) = Z P^m t^n \quad (3)$$

where, P is the discharge power, t is time and Z, m and n are empirical constant, Z is a function of the discharge length, given by

$$Z = \frac{L}{lm + 0.5N} \quad (4)$$

m=M+0.5N and n=N

where, l is discharge length.

There is no realistic and reliable model reported to determine the spark radius. In present analysis spark radius is taken as 120 μm.

H. Modeling Procedure

EDM is a complicated process that requires a powerful tool to simulate the process. In present analysis the simulation has been done on ANSYS.

In present analysis a three dimensional model of dimension 500μm×200μm×30μm has been created with sphere of 30μm diameter in it. The number of reinforced particle has been calculated by using “Rule of mixture” applied to composite materials. The element selected for analysis is tet 10 node 87.

I. Determination of material removal rate

MRR prediction depends upon the crater morphology. The morphology of crater is assumed to be spherical dome shape.

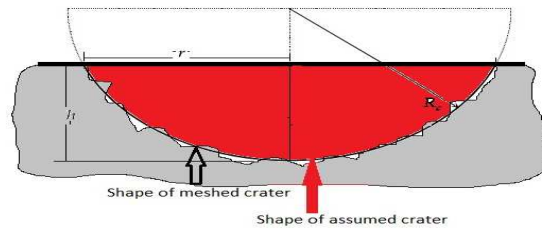


Fig. 2 Assumed crater morphology

where r is the radius of spherical dome and h is depth of dome. And the volume is calculated by given formula of spherical dome volume.

$$C_v = \frac{1}{6} \pi h (3r^2 + h^2) \quad (5)$$

The NOP can be calculated by dividing the total machining time to pulse duration as given in (6).

TABLE I
CHEMICAL COMPOSITION AND THERMAL PROPERTIES OF AL6063 AT ROOM TEMPERATURE

| Chemical Composition | | | | | | | | | |
|-----------------------------------|------------------------|-----|-----|----------|------|-----|-----|-----|-----|
| Element | Al | Cr | Cu | Mg | Fe | Mn | Si | Ti | Zn |
| Content (%) | 97.5 | 0.1 | 0.1 | 0.45-0.9 | 0.35 | 0.1 | 0.4 | 0.1 | 0.1 |
| Thermal Properties | | | | | | | | | |
| Thermal Conductivity | 210 W/mK | | | | | | | | |
| Co-efficient of Thermal Expansion | 23.4x10-6 | | | | | | | | |
| Specific Heat | 900J/kgK | | | | | | | | |
| Density | 2700 Kg/m ³ | | | | | | | | |
| Melting Temperature | 952K | | | | | | | | |
| Mechanical Properties | | | | | | | | | |
| Modulus of Elasticity | 68.9 GPa | | | | | | | | |
| Poisson's Ratio | 0.33 | | | | | | | | |
| Tensile Yield Strength | 214MPa | | | | | | | | |

TABLE II
CHEMICAL COMPOSITION AND THERMAL PROPERTIES OF SiC AT ROOM TEMPERATURE

| Chemical Composition | | |
|-----------------------------------|------------------------|--------|
| Element | SiC (Pure) | Others |
| Content (%) | 98 | 2 |
| Thermal Properties | | |
| Thermal Conductivity | 120 W/mK | |
| Co-efficient of Thermal Expansion | 4x10-6 | |
| Specific Heat | 750J/kgK | |
| Density | 3210 Kg/m ³ | |
| Melting Temperature | 3003K | |
| Mechanical Properties | | |
| Modulus of Elasticity | 415GPa | |
| Poisson's Ratio | 0.33 | |
| Tensile Yield Strength | 550MPa | |

$$NOP = \frac{T_{mach}}{T_{on} + T_{off}} \quad (6)$$

where T_{mach} is the machining time, T_{on} is pulse-on time and T_{off} is pulse-off time. Knowing the C_v and NOP one can easily derive the MRR for multi-discharge by using (7).

$$MRR = \frac{C_v \times NOP}{T_{mach}} \quad (7)$$

By using(4)-(6) material removal rate for multi-discharge with the help of single-spark model can be calculated. Table 3 shows the process parameters used for modeling [25].

III. RESULTS AND DISCUSSION

Results have been obtained for the single spark and considering Al6063/SiC as workpiece material. Temperature distribution in the workpiece has been shown in Fig. 3.

It is clearly evident from Fig. 3 that the maximum temperature occurs at the top surface on the centerline of the workpiece, where the intensity of heat flux is maximum according to Gaussian distribution of heat flux.

TABLE III
PROCESS PARAMETERS USED TO SIMULATE THE EDM PROCESS IN AL6063/SiC COMPOSITE [25]

| Properties | Value |
|---|--------------------------|
| Fraction of heat input (P) | 0.08 |
| Voltage (V) | 60 V |
| Current (I) | 9, 13 A |
| Initial temperature (T ₀) | 298 K |
| Co-efficient of heat transfer of dielectric fluid (h) | 10000 W/m ² K |
| Pulse-on time (T _{on}) | 70, 170, 270 μs |
| Pulse-off time (T _{off}) | 29, 45, 77 μs |
| Spark radius (R) | 120 μm |

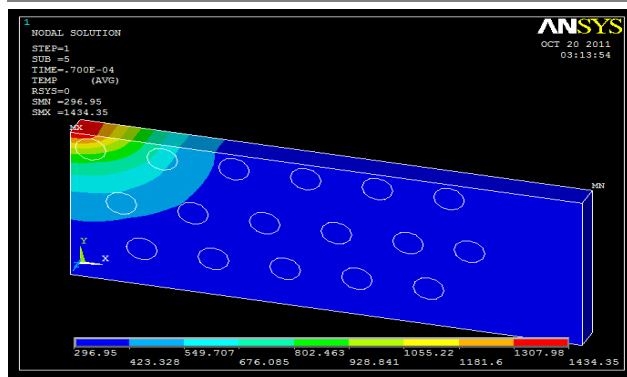


Fig. 3 Temperature distribution at the end of the single spark at V=60V, I=9A, P=0.08 and T_{on} = 70μs

Fig. 4 shows the FEA model after material removal, it is evident from the temperature distribution that, during the spark-on time the temperature rises in the workpiece and temperature rise is sufficient enough to melt the matrix due to its low melting temperature but the reinforcement remains in solid form due to its very high melting temperature. After the melting of matrix material no binding exists between the matrix and reinforcement, therefore the reinforcement evacuates the crater without getting melted.

During the pulse-off time plasma channel does not exist between the two electrodes, therefore no heat flux applied on the workpiece. During the pulse-off time only convection takes place between the workpiece and dielectric fluid.

The workpiece was assumed to be at room temperature initially, but after first discharge there is a considerable increase in the temperature of the workpiece even after the

cooling period. Fig. 5 shows the temperature distribution at the end of pulse-off time. Most of the heat is taken away by the dielectric fluid through convection and some part of heat is taken away by molten metal.

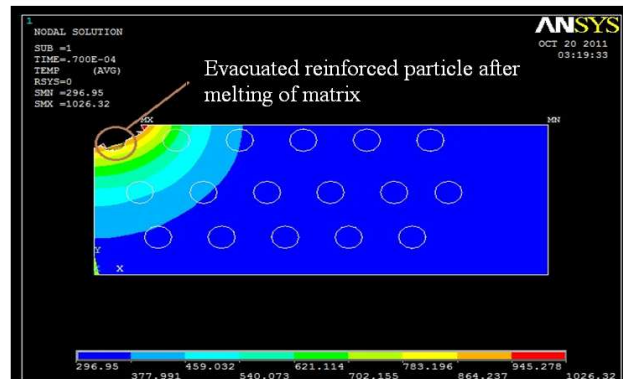


Fig. 4FEA model of Al6063/SiC composite after material removal

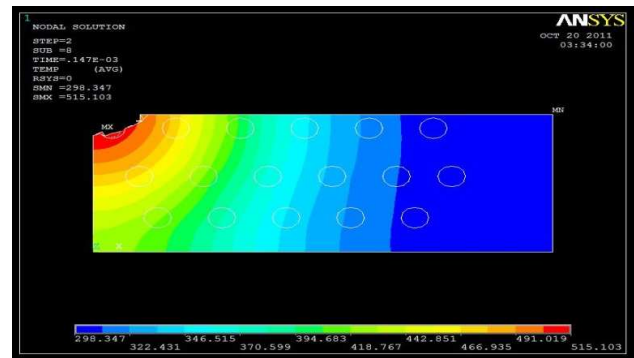


Fig. 5 Temperature distribution at the end of the pulse-off time of 77μs.

IV. FEA MODEL EXTENDED TO SECOND DISCHARGE

Simulation of second discharge pulse has also been carried out using coupled thermal structural analysis. In EDM the location of next discharge depends upon the dielectric breakdown. In present analysis, for a particular machining condition inter-electrode gap is kept constant. After first discharge slight deformation occurs causing reduction in spark gap by 0.977μm, as shown in Fig. 6.It causes the next discharge to occur at the top edge of the crater located at 60μm away from first discharge location.

Fig. 7 shows the simulated model of workpiece after second discharge. In this case the crater formed is larger than previous crater, because of the heat flux applied on the crater ridge and due to higher initial temperature. As a result the material removal rate is higher in the second discharge than that of the first discharge, but it causes poor surface finish because of the uneven crater formation.

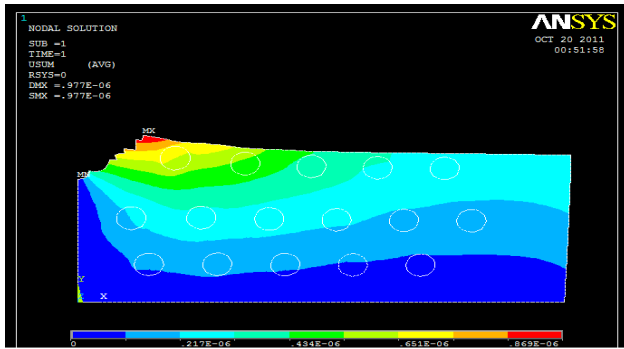


Fig. 6 Workpiece deformation after first spark

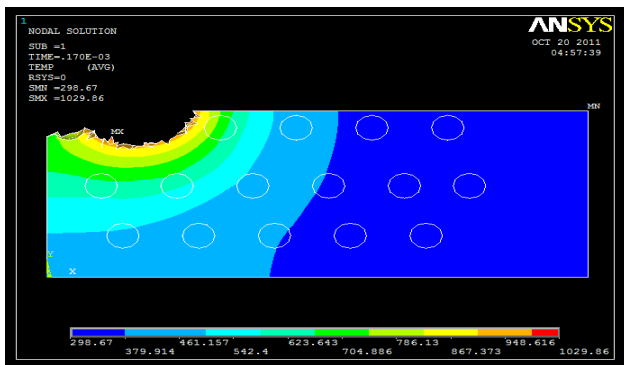


Fig. 7 Crater formation after sustained single discharge

V. MODEL VALIDATION

Model validation has been done by comparing the predicted MRR with the experimental results [25]. Fig. 8 shows the comparison between theoretical MRR and experimental values. The predicted MRR shows a coefficient of correlation of 87% with the experimental MRR. There were some deviations in the model when compared to the experimental data, this could possibly be due to some simplifying assumptions taken in the present numerical model like 100% flushing efficiency, no ignition delays, no deposition of recast layer, etc. In practice, the melted material is not fully flushed from the crater, a considerable amount of melted material again solidifies in the crater and forms the recast layer. The ideal conditions for machining are not realized due to improper flushing of debris and arcing into the inter-electrode gap during the machining with high energy discharges thus, reducing the actual MRR. The MRR is mainly influenced by spark gap, lift, sensitivity and dielectric fluid. In present analysis dielectric fluid is not playing an important role. It is coming into picture only for convection, but in actual it is a very important factor to be considered while machining. The material removal is mainly caused by melting and vaporization of material. Molten metal is taken away by the dielectric fluid, but at the same time the molten metal are under very high pressure due to plasma channel. Adhesive property of molten metal also caused problem in material removal. However, it is very difficult to model and incorporate

all these effects in the analytical model. The results reported in present analysis shows that the trends of the predicted results and experimental results are almost same.

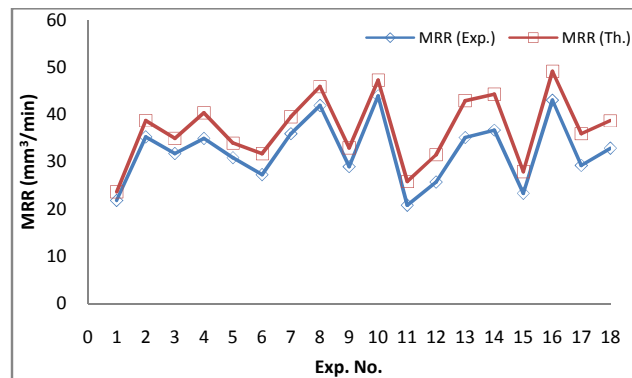


Fig. 8 Comparison of predicted MRR with experimental value

VI. CONCLUSION

In the present investigation, an axisymmetric thermal model is developed to predict the material removal rate in Al6063/SiC composite. The important features of this process such as individual material properties, shape and size of heat source (Gaussian heat distribution), percentage of heat input to the workpiece, pulse on/off time are taken into account in the development of the model. FEA based model has been developed to analyze the temperature distribution and its effect on material removal rate. To validate the model, the predicted theoretical MRR is compared with the experimentally determined MRR values. A very good agreement between experimental and theoretical results has been obtained. It is evident from the analytical model that material removal in second discharge is more than single discharge, because of initial temperature and spark occurs on crater ridge. During the EDM there is very high temperature rise in the workpiece but still it is not enough to melt the reinforced particle, so particles evacuate without melting. The model developed in present study can be further used to obtain residual stress distributions, thermal stress distribution mechanism of reinforcement particle bursting phenomenon. The follow-up publication will consider more realistic machining conditions and effects of different process parameters on the residual stress and thermal stress will be investigated. A very complex phenomenon occurs at the crater while material removal. The follow-up publications will also consider the modeling of dielectric fluid, molten material and plasma channel at the discharge crater, using CFD tool.

REFERENCES

- [1] W. König, "Machining of new materials", *Annals CIRP* vol. 39 (2), 1990, pp. 673-681.
- [2] L. Cronjäger, "Machining of fibre and particle-reinforced aluminium", *Annals CIRP* vol. 41 (1), 1992, pp. 63-66.
- [3] Allison JE and Cole GS, "Metal matrix composite in the automotive industry: opportunities and challenges", *JOM Journal of the Minerals, Metals and Materials Society*, January 1993, pp. 19-24.
- [4] J. Li, B.Y. Zong, Y.M. Wang and W.B. Zhuang, "Experiment and modeling of mechanical properties on iron matrix composites reinforced

- by different types of ceramic particles”, *Materials Science and Engineering* vol. A 527, 2010, pp. 7545–7551.
- [5] P. Narender Singh, “Electric discharge machining of Al–10%SiCp as-cast metal matrix composites”, *Journal of Materials Processing Technology*, vol. 155–156, 2004, pp. 1653–1657.
- [6] R. Komanduri, “Machining fiber-reinforced composites”, *Mech. Eng.*, April 1993, pp. 58–64.
- [7] F. Muller, “Non-conventional machining of particle reinforced metal matrix composite”, *International Journal of Machine Tools & Manufacture*, vol. 40, 2000, pp. 1351–1366.
- [8] SushantDhar, Rajesh Purohit, NishantSaini, Akhil Sharma and G. Hemath Kumar, “Mathematical modeling of electric discharge machining of cast Al–4Cu–6Si alloy–10wt.% SiCp composites”, *Journal of Materials Processing Technology*, vol. 194, 2007, pp. 24–29.
- [9] D. Kanagarajan, R. Karthikeyan, K. Palanikumar and J. Paulo Davim, “Optimization of electrical discharge machining characteristics of WC/Co composites using non-dominated sorting genetic algorithm (NSGA-II)”, *International Journal of Advance Manufacturing Technology*, vol. 36, 2008, pp. 1124–1132, DOI 10.1007/s00170-006-0921-8.
- [10] Witold We, glewski, Michal Basista, MarcinChmielewski and KatarzynaPietrzak, “Modeling of thermally induced damage in the processing of Cr–Al₂O₃composites”, *Composites: Part B*, 2011, doi: 10.1016/j.compositesb.2011.07.016.
- [11] Nilrudra Mandal, H. Roy, B. Mondal, N.C. Murmu, and S.K. Mukhopadhyay, “Mathematical Modeling of Wear Characteristics of 6061 Al-Alloy-SiCp Composite Using Response Surface Methodology”, *Journal of Materials Engineering and Performance*, DOI: 10.1007/s11665-011-9890-7.
- [12] D.S. Kumar, *Heat and Mass Transfer*, 10th edition, S.K. Kataria& Sons, Delhi, 2000.
- [13] M. Kunieda, K. Yanatori, “Study on debris movement in EDM gap, *International Journal of Electrical Machining*”, vol. 2, 1997, pp. 43–49.
- [14] Y.F. Luo, “The dependence of interspace discharge transitivity upon the gap debris in precision electro-discharge machining”, *Journal of Materials Processing Technology*, vol. 68, 1997, pp. 127–131.
- [15] K Furutani, A. Saneto, H. Takezawa, N. Mohri, H. Miyake, “Accretation of titanium carbide by electrical discharge machining with powdersuspended in working fluid”, *Precision Engineering* vol. 25, 2001, pp. 138–144.
- [16] Yih-fongTzeng and Chen Fu-chen, “A simple approach for robust design of high-speed electrical-discharge machining technology”, *International Journal of Machine Tool & Manufacture* vol. 43, 2003, pp. 217–227.
- [17] D. D. Dibitono and P. T. Eubank, “Theoretical model of the electrical discharge machining process I. A Simple Cathode erosion model,” *Journal of Applied Physics*, vol. 66, 1989, pp. 4095–4103.
- [18] M. R. Patel, B. A. Maria, P. T. Eubank and D.D. Dibitonto, “Theoretical models of the electrical discharge machining process. II. The anode erosion model,” *Journal of Applied Physics*, vol. 66/9, 1989, pp. 4104.
- [19] P. T. Eubank and M. R. Patel, “Theoretical models of the electrical discharge machining process.III. The variable mass, cylindrical plasma model,” *Journal of Applied Physics*, vol. 73/11, 1993, pp. 7900-7909.
- [20] R.Bhattacharya, V.K.Jain and P.S.Ghoshdastidar, “Numerical Simulation of Thermal Erosion in EDM Process”, *Journal of the Institution of Engineers (India), Production Engineering Division*, Vol.77, 1996, pp.13-19.
- [21] V. Yadav, V. Jain and P. Dixit, “Thermal stresses due to electrical discharge machining”, *International Journal of Machine Tools Manufacturing*, vol. 42, 2002, pp. 877–888.
- [22] P. Shankar, V.K. Jain and T. Sundarajan, “Analysis of spark profiles during EDM process”, *Machining Science Technology*, vol. 1 (2), 1997, pp. 195–217.
- [23] A. Erden, “Effect of materials on the mechanism of electric discharge machining (EDM)”, *Transactions of ASME, Journal of Engineering Materials and Technology* vol. 108, 1983, pp. 247–251.
- [24] K. Salonitis, A. Stourmaras, P. Stavropoulos and G. Chryssolouris, “Thermal modeling of the material removal rate and surface roughness for die-sinking EDM”, *International Journal of Advanced Manufacturing Technology*, vol. 40, 2009, pp. 316 – 323.
- [25] A. Divedi “Experimental investigation and optimisation in EDM of Al 6063 SiCp metal matrix composite”, *International Journal of Machining and Machinability of Materials*, Vol. 3, Nos. 3/4, 2008, pp. 293-308.